COMPUTATIONAL MODELLING OF SELF-CENTERING PRECAST CONCRETE WALLS

Jonathan Watkins[1], Richard S. Henry[1], and Sri Sirtharan[2]

[1] The University of Auckland
20 Symonds Street, Auckland 1010, New Zealand
jwat133@aucklanduni.ac.nz ; rs.henry@auckland.ac.nz

[2] Iowa State University
406 Town Engineering Building, Ames, IA 50011, USA
sri@iastate.edu

Keywords: concrete wall, unbonded post-tensioned, modelling, analysis, self-centering, rocking.

Abstract. *Existing predictive models of self-centering precast concrete walls with post-tensioning are generally computationally expensive. While simplistic models have a low computational cost, they are generally incapable of simulating cyclic behavior of these walls. Hence, a new computational model suitable for characterizing cyclic response of self-centering precast concrete walls was developed with emphasis on accuracy and computational efficiency. The proposed model consisted of a bed of truss elements at the base of wall where the rocking response is expected, truss elements for the post-tensioning tendons, and an elastic beam-column element for the wall panel. To ensure the accuracy of wall response, including the quantification of residual displacements, a robust concrete hysteresis model was required in the analysis. The proposed modelling technique was verified against five experimental tests completed on self-centering precast concrete walls. In all cases, the model accurately captured the overall cyclic behavior and residual displacements of the self-centering precast concrete wall. Furthermore, the models also satisfactorily captured several local response parameters, including the wall uplift, neutral axis depth, lateral drifts at which concrete spalling and crushing occurred, and post-tensioning force for both loading and unloading cycles at all ranges of lateral drifts.*

1   INTRODUCTION

Self-centering precast concrete walls are generally designed with unbonded post-tensioned (PT) tendons. Due to their low energy dissipating ability, additional energy dissipation for these walls can be provided by supplemental energy dissipating elements. Self-centering precast concrete walls allow for safe dissipation of energy imparted to the building by an earthquake motion while incurring minimal structural damage. Previous experimental and analytical research has shown that these walls can be designed to produce excellent seismic performance [1, 2].

The prediction of self-centering precast concrete walls behavior and performance when subjected to seismic excitation is critical for their implementation into buildings. Existing computational models developed for self-centering precast concrete walls are often computationally expensive, or reduce the computational demand with model simplifications that degrade the accuracy of the analysis. A summary of available computational modeling techniques for self-centering precast concrete walls is first presented. The development of a new, efficient computational model with a capability of simulating the cyclic behavior of self-centering precast concrete walls is then reported. Finally, the proposed computational modelling technique is verified against available experimental results and the results are discussed.

2   BACKGROUND

Previous research in the modelling of cyclic behavior of self-centering precast concrete walls has led to the development of several computational techniques using the finite element method (FEM) in various forms including those based on solid brick, fiber-based, multi-spring macro and lumped plasticity elements. Lumped plasticity models, in the form of non-linear rotational springs, have a low computational demand and are the simplest computational technique. Several researchers have used this element to model self-centering precast concrete walls [e.g., 3-5]. In general, these models showed satisfactory agreement with the overall experimental response. However, two disadvantages of non-linear rotational springs were found. In most cases, the springs were limited in their ability to capture the cyclic behavior. In one case that characterized the cyclic response, the lumped plasticity models parameters were calibrated using the measured experimental results.

Multi-spring macro-models have increased computational cost but do not suffer from the deficiencies noted earlier. These models capture the wall's rocking motion with a bed of compression only axial springs at the wall-to-foundation interface, and truss elements represent the post-tensioning. This approach can explicitly account for the hysteric energy dissipation from the inelastic strains in the concrete and post-tensioning. Researchers using this model have adequately captured the cyclic behavior of self-centering precast concrete walls [5-7]. The accuracy of the wall response was increased when a greater number of axial springs were used to represent the wall-to-foundation interface.

In contrast to the previous models, fiber and solid brick models capture the spread of strains along the height of the wall. This enables all aspects of the walls to be accurately captured but the computational cost is high. Many researchers have used fiber or solid brick models to characterize the response of self-centering precast concrete walls [4, 8-14]. Overall the behavior of the wall was well captured using fiber models, with further improvements resulting from the use of models based on brick elements.

The reported differences between these models can be seen in the analyses published on the same experimental test of a self-centering precast concrete wall [5, 7, 9]. The non-linear rotational spring model failed to accurately capture the hysteretic actions, which were adequately characterized by both the multi-spring and fiber section models. These analyses ap-

pear to validate that an average strain at the wall base can be used to determine the wall's resistance and energy dissipation characteristics. The high rate of change of curvature, and therefore strain, at the wall base is thought to allow this simplification. This model can have comparable accuracy to that of fiber section models, which does not use this simplification.

3 PROPOSED COMPUTATIONAL MODEL

The proposed computational model, shown in Figure 1, is an amalgamation of the fiber section and multi-spring models. It retains the accuracy of the fiber section model and the low computational demand of the multi-spring model. The model contains three elements: a bed of truss elements representing the rocking interface, truss elements representing the post-tensioning tendons, and an elastic beam-column element representing the wall panel. The truss elements are fixed at the base and connected via rigid links to the base of the elastic beam-column element. Therefore, the deformation of the truss elements, which represents the wall uplift and toe compression, is only a function of the wall's rotation. In using this technique to model the rocking wall interface, two assumptions are made: inelastic action of the concrete wall panel is concentrated at the rocking interface, and the wall uplift and toe compression depend only on the wall panel's rotation. Henry *et al*. [13] found both experimentally and analytically that the wall panel behaved elastically a short distance above the single horizontal crack located at the wall base, and therefore using an elastic beam-column element to represent the wall panel above the wall-to-foundation interface is acceptable. As previously discussed, using an average strain at the wall base, i.e. the bed of truss elements, can adequately capture the energy dissipation of the wall panel. Perez *et al*. [11] have presented equations to calculate the height of the truss elements at the wall base, which allowed the truss elements to correctly capture the spalling and crushing of concrete at a comparable drift to experimental results.
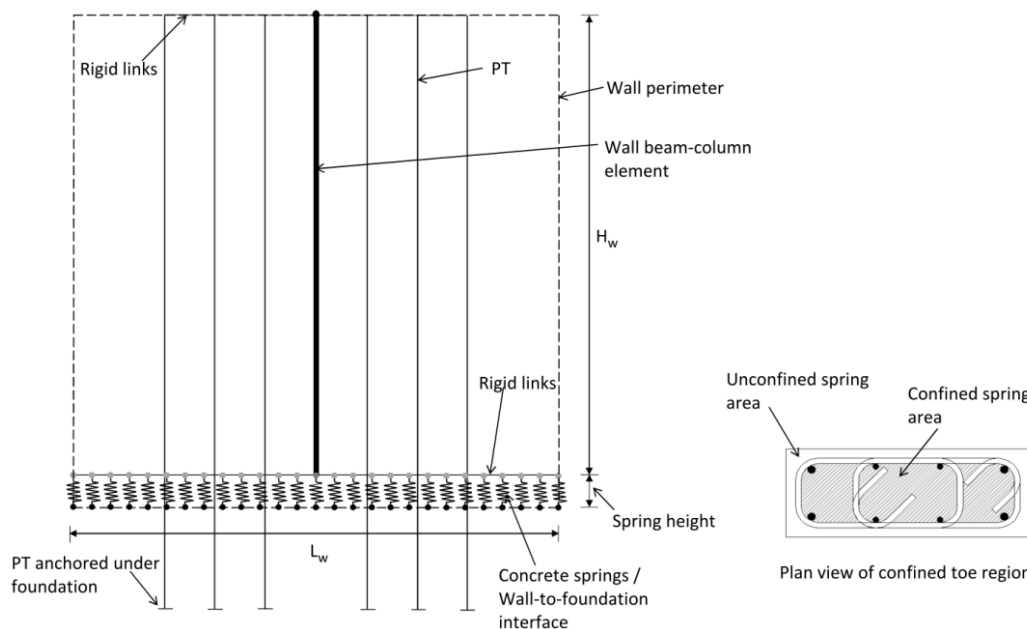

Figure 1: General layout of the proposed computational model

An analysis of several experiments on self-centering precast concrete walls showed strong evidence that the wall uplift is a function only of the rotation at the base of the wall panel [1, 12, 15]. In the self-centering precast concrete wall experiment conducted by Aaleti *et al.* [1],

LVDT's were used to measure the uplift along the base of the wall, and strain guages were used to measure the toe compression. The experimental uplift of the wall base was compared to the uplift calculated using the wall base rotation. This comparision confirmed that there was a 94.7% fit to the hypothesis that the wall uplift is a function of the wall base rotatation, and for lateral drifts greater than 0.5%, the corresponding accuracy increased and resulted in 99.6% fit. Furthermore, the analysis showed the toe compressive strains followed a triangular distribution, which is used in the proposed computational model.

For the bed of truss elements at the wall base in the proposed model the required inputs are length, area, and uniaxial material model. The element length can be calculated from recommendations by Perez *et al.* [11], where the minimum of either twice the walls' neutral axis depth at failure, or twice the width between the centerlines of toe confinement reinforcement was suggested. The area of the spring is dependent of its location. In unconfined regions, the spring's area is equal to the wall's width multiplied by the spring spacing. In the confined toe region two springs are used, one for the confined region and the other for the unconfined cover region, and the areas calculated from construction drawings as illustrated in Figure 1.

The uniaxial concrete stress-strain material model for the truss elements was established from research by Waugh [16], and Chang and Mander [17]. Waugh implemented a unidirectional cyclic concrete material model, known as Concrete07, into OpenSees [18], which was based on Chang and Mander's concrete model that is applicable to both confined and unconfined concrete. The response envelope of the Chang and Mander's model is the same as that proposed by Mander et al. [19], which has been extensively used in analytical research. The use of Waugh's uniaxial concrete material model has improved the accuracy of analytical models of experimentally tested reinforced concrete walls in comparison to other existing uniaxial concrete material models [16]. The increased accuracy was attributed to Chang and Mander's degrading unloading stiffness.

With further simplifications to Concrete07, a compression only uniaxial concrete material model was established in OpenSees, as this is more suitable for modeling concrete at the base of a rocking wall. Figure 2 shows the typical loading, unloading and reloading path of the modified Concrete07, with numbers 1 through 6 illustrating various paths. Number 1 is the Chang and Mander's envelope. When loading at strains greater than ε_{cc}, representing the strain at maximum concrete stress, there is an option to continue with Chang and Mander's envelope, or follow a user defined linear backbone by specifying (ε_u, f_u). Numbers 2 to 5 illustrate various unloading and reloading options, with the simplest definition being unloading and reloading paths with the initial stiffness E_c (i.e, 2a) or degraded stiffness E_{sec} (i.e., 2b). Unloading along the response curve and reloading with E_{sec} (2, 5) has a high computational cost due to the large number of iterations required for the model to converge. To reduce the computational cost, Waugh proposed a tri-linear approximation of the Chang and Mander unloading curve based on the initial and final stiffness of unloading (2c). The tri-linear unloading path introduced convergence errors because at large strains the final stiffness is a small fraction of the initial stiffness. Hence, a bi-linear unloading option was implemented in the modified Concrete07, illustrated by path 2d. As seen in Figure 2, the model unloads from, and reloads to the same strain, ε_{un}, whereas Chang and Mander's model reloads to a slightly greater strain. This modification was adopted by Waugh and in the modified Concrete07 to further minimize convergence errors. Paths 3 to 5 illustrate the compression only nature of the concrete model. Once the model has unloaded to a strain of ε_{pl}, there is no increase in stress until a strain greater than ε_{pl} is reached. Number 6 shows after reloading to a strain of ε_{un} the concrete model follows the envelope option previously specified. The strain ε_{sp} sets the concrete crushing strain. Once this strain is met, the concrete is assumed to provide no further resistance, returning zero stresses for all strains.
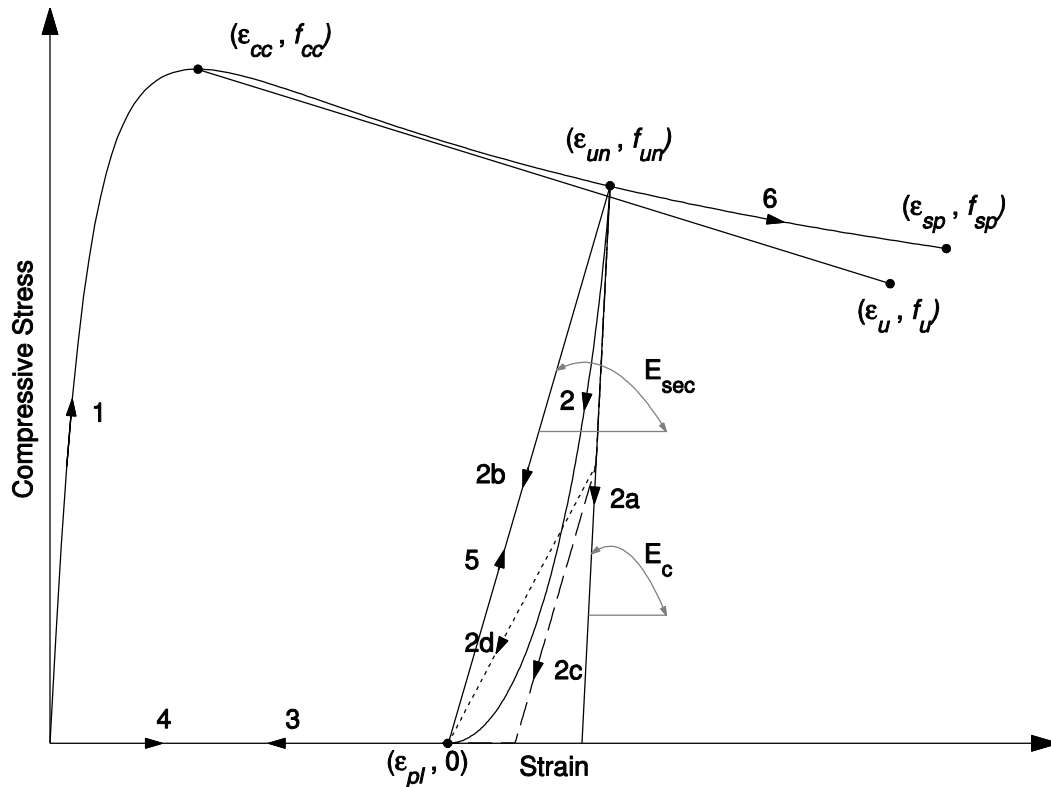
Figure 2: Stress-Strain definition of modified Concrete07 representing compression only uniaxial behavior

4   EXPERIMENTAL VALIDATION

A set of experimental tests were used to validate the proposed computational model. Perez *et al.* [11, 12] conducted an experimental program into the behavior of multistory concrete walls utilizing unbonded post-tensioned tendons. The five wall tests were conducted by representing a prototype wall approximately at half scale, and included the bottom four stories of the six story wall. The test walls were subjected to quasi-static monotonic and cyclic lateral loads, and the average total gravity load was 3.7% of $f_c'A_g$. Four parameters were changed between the five test walls: type of confinement reinforcement, initial stress in the PT bars, f_{pi}, initial concrete stress due to post-tensioning, $f_{ci,p}$, and total area of the PT tendons, A_p. These parameters are summarized in Table 1 and further details are reported by Perez *et al.*

The model layout used in the analysis was shown previously in Figure 1. The lateral displacement was applied at a height of 7.23 m from the wall base, and the unbonded tendon length was 9.91 m. There were seven oversized ducts 70 mm in diameter in the wall panel and the PT was 32 mm in diameter. Elastic beam-column elements were used to represent the concrete wall panels. The material stress-strain inputs for the bed of truss elements shown in Figure 3a and 3b were based on cylinder tests conducted by Perez *et al*. A bed truss height of twice the width between the centerlines of toe confinement reinforcement was used. However, the bed truss height of TW5 was increased by 40% to prevent confined crushing occurring in the computational model, reflecting the experimental results. Confined concrete crushing did not occur in TW5 due to the smaller area of PT, which decreased the toe compressive forces. Alternatively, to match the experimental lateral drift at which concrete crushing occurred, Perez *et al's.* cyclic analysis kept the fiber's height constant, and adjusted the concrete crushing strain in the material. Given the discrepancies in capturing the lateral drift when concrete crushing occurs, further analysis is required to establish predictive equations for the truss height. In the proposed model the spacing between truss elements representing the rocking at

the wall base was set at L_w/1000, i.e. 2.54 mm. The relatively small spacing was required to minimize any convergence issues, which can be triggered by a reduction in a truss elements stress that cannot be redistributed to adjacent elements because of the large spacing.

Table 1: Test matrix from Perez *et al.* [11]

Test wall	Loading	A_p (cm^2)	f_{pi}/f_{pu}	$f_{ci,p}$ (MPa)	Confinement Type	PT bars
TW1	Monotonic	48.4	0.553	8.20	Spirals	xx xox xx
TW2	Cyclic	48.4	0.553	8.20	Spirals	xx xox xx
TW3	Cyclic	48.4	0.553	8.20	Hoops	xx xox xx
TW4	Cyclic	48.4	0.277	4.07	Hoops	xx xox xx
TW5	Cyclic	24.2	0.553	4.07	Hoops	xo oxo ox
*x = bar and o = empty duct						

a) Concrete stress-strain for TW1 & TW2

b) Concrete stress-strain for TW3-TW5
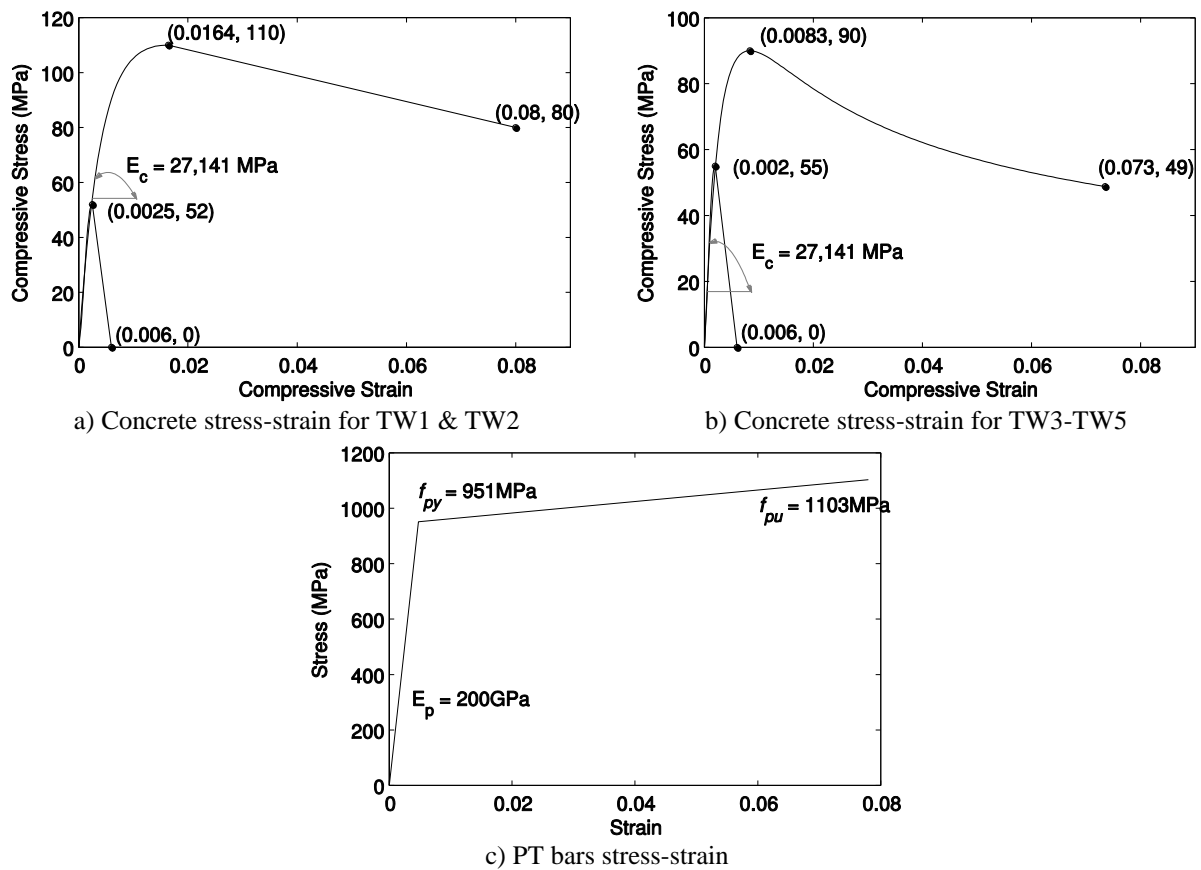

c) PT bars stress-strain

Figure 3: Material properties used for the analyses, based on experimental testing by Perez *et al.* [12]

5   RESULTS

Figures 4-9 compare the analytical results from the new model to the experimental test results for all five test walls, referred to as TW1 to TW5. Figure 4a compares the experimental results of the base shear versus lateral drift with the analytical results for TW1. This comparison shows the initial stiffness and decompression of the wall were closely matched. It also shows the spalling (SPL) and crushing of concrete (CCC) were closely captured at 0.6% and

3.5% lateral drifts, respectively, so is the yielding of the PT at 1.5% lateral drift. However, the base shear is slightly overestimated after yielding of the PT steel. In addition, Figure 4b shows the analytical model closely matched the uplift of the wall at the west wall edge and at the center of the wall.
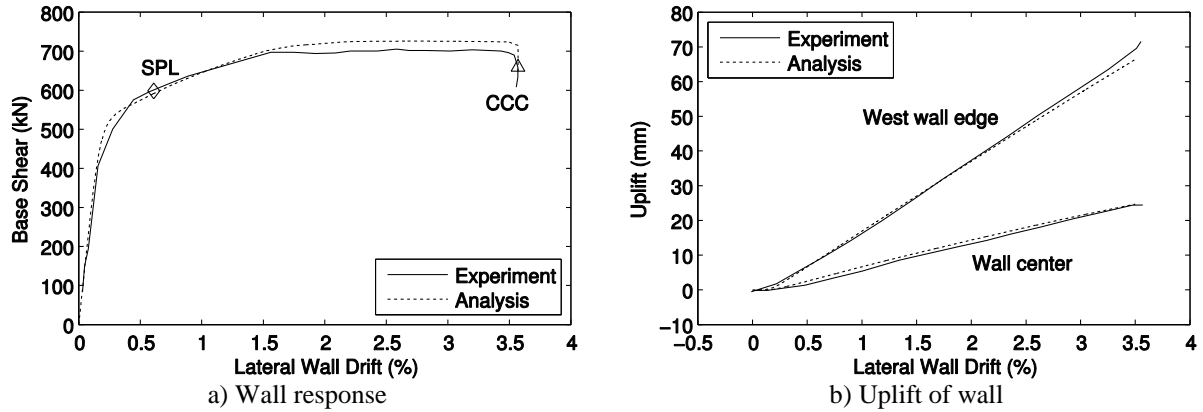

a) Wall response

b) Uplift of wall

Figure 4: Comparison between experimental and analytical results for TW1

TW2 had identical parameters to TW1, except that it was subjected to cyclic loading. Figure 5a shows the analytical loading and unloading hysteresis loops are in good agreement with the experimental results. Figure 5a also shows the experimental residual drifts were well captured. Figures 5c and 5d confirm that the yielding of PT1 and PT3 which occurred at 1.5% and 2.1% drifts were accurately captured. Figure 5b also shows the analytical model closely matched the uplift of both wall ends.

a) Wall response

b) Uplift of wall

c) Normalised stress in PT1
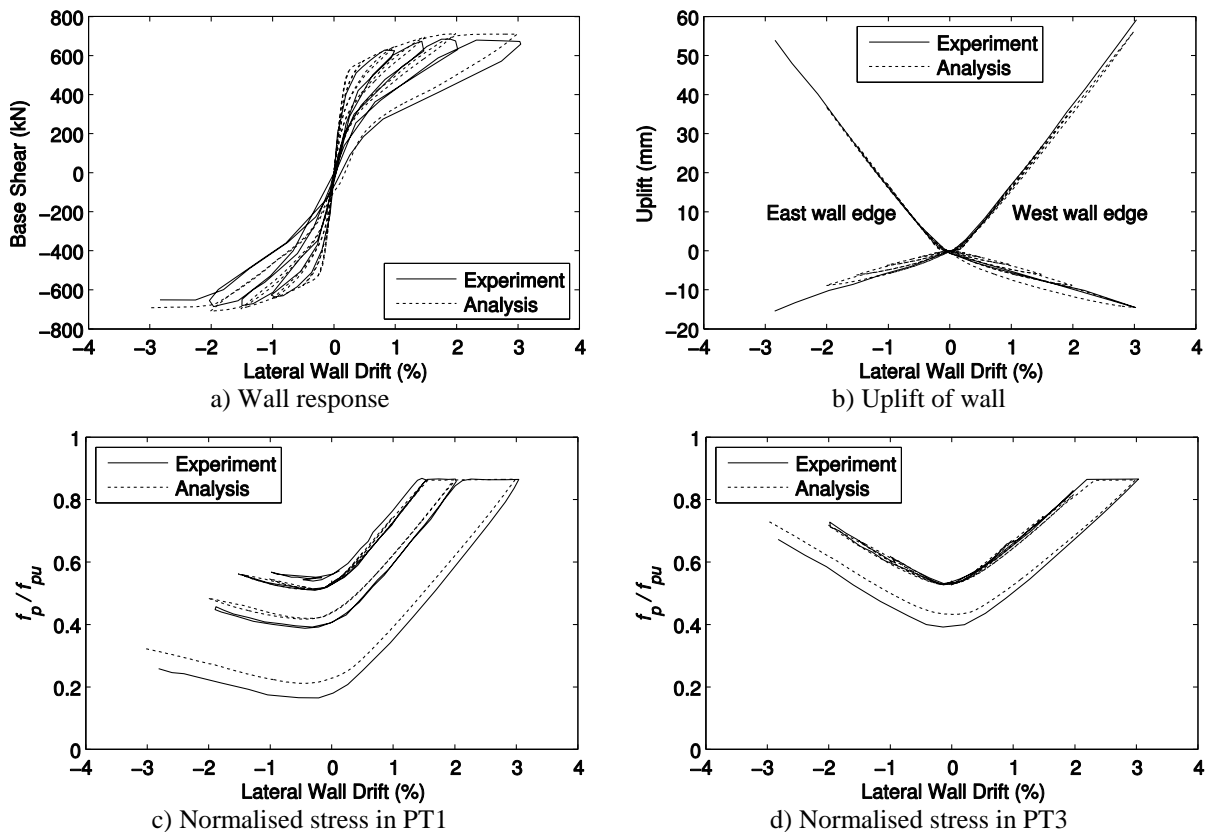
d) Normalised stress in PT3

Figure 5: Comparison between experimental and analytical results for TW2

TW3 differed from TW2 and TW1 by using hoop rather than spiral reinforcement in the wall toe confinement region. TW3's experimental lateral load response shows early spalling of the concrete at the west wall end at 0.57% lateral drift as seen in Figure 6a, which was attributed to poor consolidation of concrete during casting [12]. Furthermore, the unsymmetrical nature of the experimental results led to an accumulated negative drift of 0.1%. The analytical results presented in Figure 6 do not reflect this behavior because the model was based on symmetrical properties of the test wall. A comparison between the experimental and analytical lateral load response of TW3, shown in Figure 6a, shows the results are generally in good agreement, and in some agreement for the hysteresis loops obtained for the east end. The comparison also shows the loss of strength in the east direction of the wall at 3% lateral drift indicating that concrete crushing was accurately captured. Convergence errors arose when crushing of the confined concrete occurred. Figures 6c and 6d show that the yielding of PT1 and PT3 were closely matched, while Figure 6b shows the wall uplift was closely captured until crushing of the confined concrete occurred.

a) Wall response

b) Uplift of wall

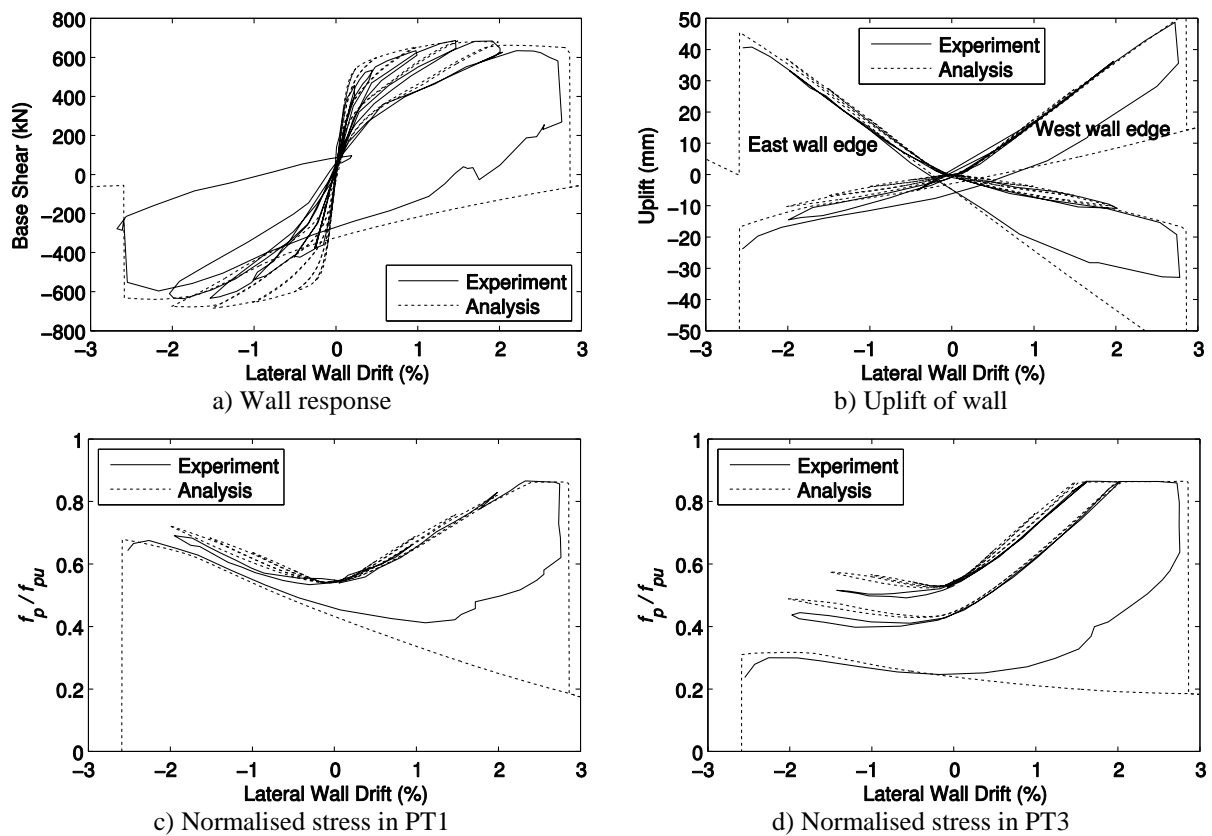c) Normalised stress in PT1

d) Normalised stress in PT3

Figure 6: Comparison between experimental and analytical results for TW3

TW4 was intended to quantify the effect of reducing the initial stress in the PT on the wall response. Figure 7a compares the base shear versus lateral drift obtained from the test and that calculated by the analytical model for TW4. The comparison again shows good agreement until the experimental lateral resistance progressively weakened after a lateral drift of 3%. Unlike the previous walls, TW4 retained some of its lateral resisting capacity after experiencing crushing of the confined concrete, suggesting that the uniaxial concrete stress-strain model requires some modifications to capture the residual strength of the concrete after rupture of the confinement reinforcement. Figure 7b shows the wall uplift was accurately captured for

lateral drifts up to 3%; Figures 7c and 7d show generally good agreement between the analytical and experimental PT stresses for lateral drifts up to 3%.

a) Wall response

b) Uplift of wall

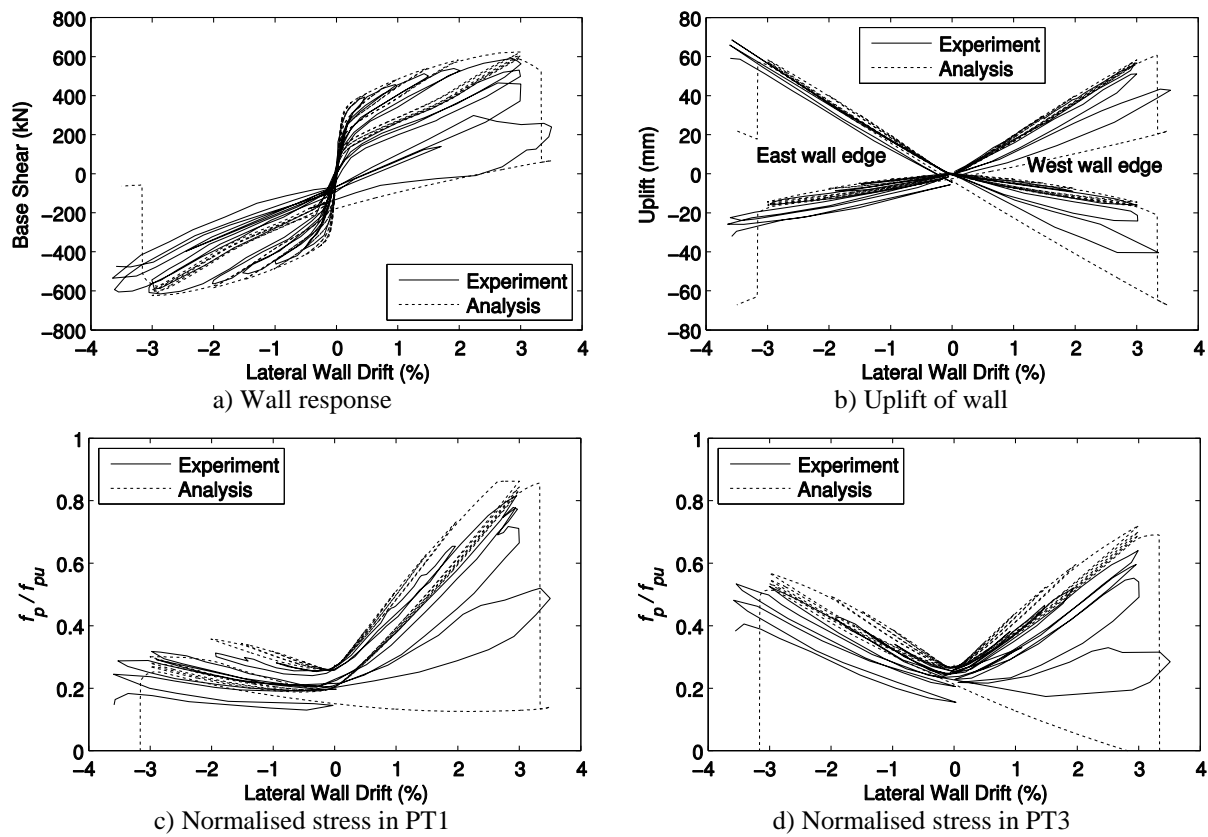c) Normalised stress in PT1

d) Normalised stress in PT3

Figure 7: Comparison between experimental and analytical results for TW4

The purpose of TW5 was to quantify the effect of reducing the total area of PT steel, A_p, while maintaining the initial stress in the PT and at the wall base. During the experiment, PT1 and PT3 lost all of their initial pre-stress due to yielding occurring at a high drift of about 5%. To prevent the truss elements representing the PT from resisting compressive stresses, a tension only element was placed in series with the PT truss. Figure 8a shows very good agreement between the experimental and analytical results of the base shear versus lateral drift. Figure 8b shows the wall uplift was accurately quantified, while Figures 9a and 9b show PT stresses were closely matched, but with some discrepancy on the final cycle at 6% lateral drift.
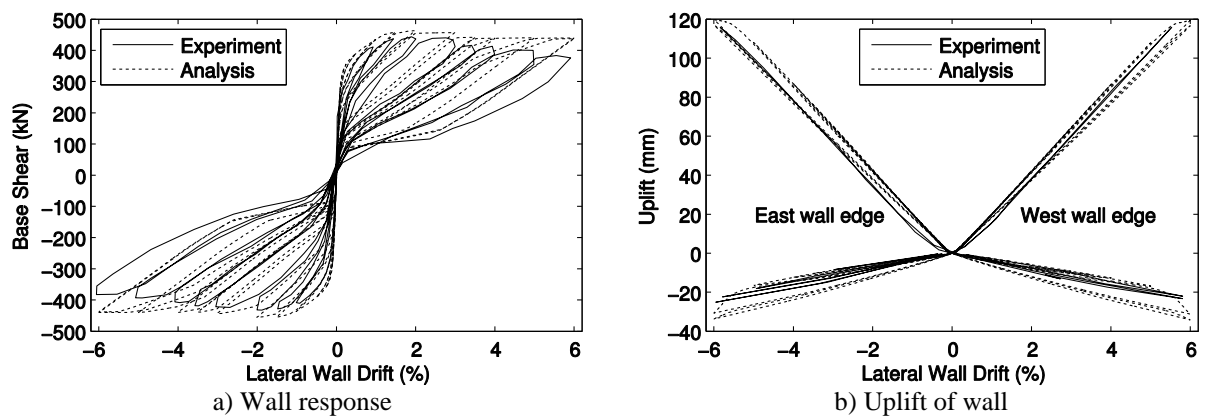

a) Wall response

b) Uplift of wall

Figure 8: Comparison between experimental and analytical results for TW5

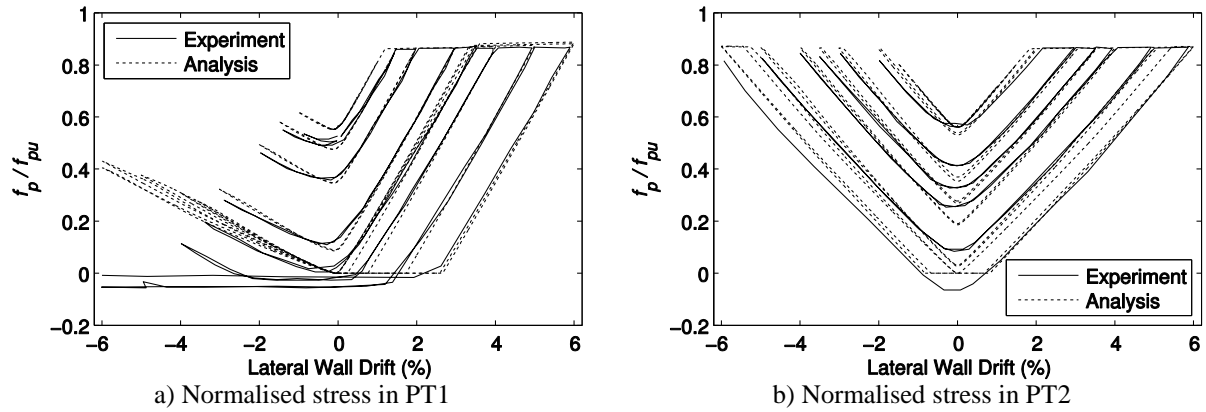a) Normalised stress in PT1   b) Normalised stress in PT2

Figure 9: Comparison between experimental and analytical results for TW5

6 CONCLUSIONS

After identifying lack of computationally efficient models for quantifying nonlinear cyclic behavior of self-centering precast concrete walls, a new computational model was presented. The proposed model comprised of: a bed of truss elements to capture the wall-to-foundation rocking interface, truss elements for the PT, and elastic beam-column elements for the wall panel. A robust uniaxial concrete stress-strain model was used to increase the accuracy of the analytical simulation, including accurate capture of residual displacements. The model was validated using five tests reported on self-centering precast concrete walls. The following conclusions were drawn from this investigation:

- The computational model showed very good agreement with the non-linear cyclic behavior of the self-centering precast concrete walls. The model accurately captured the inelastic energy dissipated by the rocking behavior and inelastic elongation of the post-tensioning.
- The model had a low computational cost and has the ability to predict the cyclic behavior of self-centering precast concrete walls.
- The bed of truss elements using the uniaxial concrete stress-strain material model accurately captured the wall-to-foundation rocking interface, including residual displacements. The concrete stress-strain material model allowed the computational model to closely capture the lateral drifts at which concrete spalling and confined concrete crushing occurred. A truss bed height of twice the width between the centerlines of toe confinement reinforcement is recommended.
- The model closely estimated the wall uplift and change in neutral axis. The stress in the post-tensioning was comparable to the experimental results, however, the stress was slightly over estimated in some cases.

In the process of validating the proposed model, the following areas were identified for improvements: 1) calculating the bed height and spacing of truss elements; 2) characterizing wall behavior after crushing of confined concrete; and 3) a further refinement to the estimation of PT stresses. Further research will be conducted to overcome these challenges in the proposed computational model.

7 ACKNOWLEDGEMENTS

REFERENCES

1. Aaleti, S. and S. Sritharan, *Performance Verification of the PreWEC Concept and Development of Seismic Design Guidelines*, 2011, ISU-CCEE Report 02/11 Iowa State University.

2. Priestley, M.J.N., S.S. Sritharan, J.R. Conley, and S. Pampanin, *Preliminary results and conclusions from the PRESSS five-story precast concrete test building.* PCI Journal, 1999. **44**(6): p. 42-67.

3. Rahman, M.A. and S. Sritharan, *An evaluation of force-based design vs. direct displacement-based design of jointed precast post-tensioned wall systems.* Earthquake Engineering and Engineering Vibration, 2006. **5**(2): p. 285-296.

4. Henry, R.S., *Self-centering Precast Concrete Walls for Buildings in Regions with Low to High Seismicity*, 2011, PhD Thesis, University of Auckland.

5. Palermo, A., S. Pampanin, and A.J. Carr, *Efficiency of simplified alternative modelling approaches to predict the seismic response of precast concrete hybrid systems*, in *fibSymposium 2005: "Keep Concrete Attractive"* 2005: Budapest, Hungary.

6. Conley, J., S. Sritharan, and M.J.N. Priestley, *Precast Seismic Structural Systems PRESSS-3: The Five-Story Precast Test Building Vol. 3-1: Wall Direction Response*, 2002, Report No. SSRP-99/19: University of California, San Diego.

7. Pennucci, D., G.M. Calvi, and T.J. Sullivan, *Displacement-based design of precast walls with additional dampers.* Journal of Earthquake Engineering, 2009. **13**(1): p. 40-65.

8. Kurama, Y., R. Sause, S. Pessiki, and L.W. Lu, *Lateral load behavior and seismic design of unbonded post-tensioned precast concrete walls.* ACI Structural Journal, 1999. **96**(4): p. 622-632.

9. Smith, B.J. and Y.C. Kurama. *Design of hybrid precast concrete walls for seismic regions*. in *2009 Structures Congress*. 2009. Austin, TX, United States.

10. Erkmen, B. and A.E. Schultz, *Self-centering behavior of unbonded, post-tensioned precast concrete shear walls.* Journal of Earthquake Engineering, 2009. **13**(7): p. 1047-1064.

11. Perez, F.J., R. Sause, and S. Pessiki, *Analytical and experimental lateral load behavior of unbonded posttensioned precast concrete walls.* Journal of Structural Engineering, 2007. **133**(11): p. 1531-1540.

12. Perez, F.J., *Experimental and Analytical Lateral Load Response of Unbonded Post-Tensioned Precast Concrete Walls*, 2004, PhD Thesis, Lehigh University.

13. Henry, R.S., N.J. Brooke, S. Sritharan, and J.M. Ingham, *Defining concrete compressive strain in unbonded post-tensioned walls.* ACI Structural Journal, 2012. **109**(1): p. 101-112.

14. Kurama, Y.C., *Seismic design of unbonded post-tensioned precast concrete walls with supplemental viscous damping.* ACI Structural Journal, 2000. **97**(4): p. 648-658.

15. Twigden, K.M., R.S. Henry, and Q.T. Ma, *Dynamic testing of post-tensioned rocking walls*, in *15th World Conference on Earthquake Engineering* 2012: Lisbon,Portugal.

16. Waugh, J.D., *Nonlinear analysis of T-shaped concrete walls subjected to multi-directional displacements*, 2009, PhD Thesis, Iowa State University.

17.   Chang, G.A. and J.B. Mander, *Seismic Energy Based Fatigue Damage Analysis of Bridge Columns: Part 1 - Evaluation of Seismic Capacity*, 1994, State University of New York, Buffalo, NY: NCEER Tehcnical Report No. NCEER-94-006.

18.   Mazzoni, S., F. McKenna, M.H. Scott, and G.L. Fenves, *Open System for Earthquake Engineering Simulation*, 2006, Pacific Earthquake Engineering Research Center, University of California, Berkeley.

19.   Mander, J.B., M.J.N. Priestley, and R. Park, *THEORETICAL STRESS-STRAIN MODEL FOR CONFINED CONCRETE.* Journal of Structural Engineering New York, N.Y., 1988. **114**(8): p. 1804-1826.